Flow, Turbulence and Combustion (2024) 112:1105–1126
https://doi.org/10.1007/s10494-024-00530-w

RESEARCH

A Detailed Analysis of Mixture Stratification on Flame Displacement Speed for Syngas Combustion

Rahul Patil[1] · **Sheshadri Sreedhara**[1]

Received: 11 September 2023 / Accepted: 8 January 2024 / Published online: 3 February 2024

Abstract

Gasoline direct injection engines can provide higher thermal efficiency and lower emissions than that for engines using conventional combustion techniques. Compositional stratification inside the combustion chamber opens possibilities for ultra-lean and low-temperature combustion. To explore this further, 2D direct numerical simulation (DNS) has been performed to investigate the propagation of syngas flame in an equivalence ratio (ϕ) stratified medium. Several aspects of flame propagation, such as effect of integral scale of mixing (l_ϕ) on the non-monotonic behavior of flame propagation, contribution of each chemical reaction to heat release rate (HRR), and the effect of differential diffusion were analyzed using DNS-data. A spherically expanding flame has been initiated with a hotspot at the center of the square domain of size 2.4×2.4 cm^2. The variations in the degree of stratification were simulated varying l_ϕ and fluctuations ϕ for initial mixture distribution. Further this DNS-data has been used to analyze effects of stratification on flame displacement speed (S_d) and its components, viz. reaction rate (S_r), normal diffusion (S_n), tangential (S_t), and inhomogeneity (S_z). The results reveal that stratification-induced variations in thermal diffusivity resulted in thermal runaways. These thermal runaways influence the extent of burning for simulated cases. The increase in degree of stratification resulted in flame preferably propagating towards leaner ϕ, causing reduction in components of S_d. The preferential propagation of flame also resulted in shifting of peak reaction rate for fuel species (c^*) to a higher reaction progress variable (c). This shifting of c^*, lead to a reduction in the HRR contribution of reactions that attain their peak near the production zone of H and OH species. For unity Le simulations, S_n was observed to be reduced drastically compared to cases with differential diffusion, resulting in an overall reduction in S_d.

Keywords Direct numerical simulations (DNS) · Compositional stratification · Displacement speed · Syngas

✉ Sheshadri Sreedhara
sreedhara.s@iitb.ac.in

[1] IC Engines and Combustion Laboratory, Department of Mechanical Engineering, Indian Institute of Technology Bombay, Mumbai 400076, India

1 Introduction

With rising concern over emissions and fuel prices, providing efficient combustion with low carbon emissions are the major challenges for combustion researchers. The combustion in practical combustion devices primarily takes place by either premixed or diffusion mode. Both operating modes have their own merits and demerits. Premixed combustion is usually clean in terms of unburnt hydrocarbon emissions compared to diffusion combustion (Ilbas and Karyeyen 2017). But, reduced combustion efficiency at part load operation is a well-known challenge for premixed combustion (Manente et al. 2011). Using a compositionally stratified mixture inside the combustion chamber is one method to improve part load performance for combustion systems using a premixed mode of operation. Compositional stratification is an integral part of new combustion technologies such as Low-Temperature Combustion (LTC), Homogeneous Charge Compression Ignition (HCCI), Moderate and Intense Low-oxygen Dilution (MILD), etc. The compositional stratification is generally achieved in engines using direct injection inside the combustion chamber (Agarwal et al. 2023; Tan et al. 2016; O'Donnell et al. 2023) or by dilution of the fuel–air mixture (Telli et al. 2022; Fooladgar and Chan 2017; Zhao et al. 2019). With stratification, stoichiometric or slightly rich mixtures can be used near the ignition source, and ultra-lean mixtures can be used near the chamber walls. This layering in fuel composition helps to increase part load efficiency and avoid the possibility of knocking (Bai et al. 2013). By utilizing a stratified mixture, the flammability limits can be widened for engine operations (Kang and Kyritsis 2005).

Despite these potential benefits, fundamental studies for stratified combustion are sparse. In experimental studies, difficulties lie in reproducing inhomogeneity in partially premixed mixtures and relating it to diagnosis associated with these turbulent flames. The main emphasis of these experimental studies is to relate flame propagation behavior to stratification. Past experimental studies (Kang and Kyritsis 2005; Aleiferis et al. 2005; Cho et al. 1992; Costa et al. 2018) suggested that the cyclic variations during combustion are significantly more for stratified mixtures than the uniformly premixed cases. Further, a significant increase in flame wrinkling was observed due to the stratification. The misfire rate was observed to increase significantly with an increase in the root mean square (*rms*) value of equivalence ratio fluctuations (ϕ'). Zhou et al. (Zhou et al. 1998) showed that flame propagation behaves non-monotonically with an increase in the degree of inhomogeneity. The flame propagation speed was also dependent on the value of the mean equivalence ratio of the fuel–air mixture. This dependence becomes weaker with a further increase in inhomogeneity in the mixture. A significant increase in flame propagation speed and enhancement of flammability limits was reported for mixtures with lean compositions (Kang and Kyritsis 2005). This enhancement was traced back to excessive heat released by the rich fuel packets in the domain.

Due to fewer approximations, Direct Numerical Simulations (DNS) studies give better insight into the physics of a process. Few studies suggested that increase in mixture inhomogeneity increases the flame surface area and flame temperature e.g. (Jiménez et al. 2002). This increase in flame temperature leads to increased efficiency and NO production. For mixtures with lean compositions, a significant enhancement in flame propagation speed and wider flammability limits were reported with introduction of stratification (Kang and Kyritsis 2005). This enhancement was traced back to excessive heat released by the rich fuel packets in the domain. Along with these results, multiple studies reported the non-monotonic behavior of flame propagation with increased inhomogeneity. A study by Patel and Chakraborty (Patel and Chakraborty 2014) showed that with an increase in ϕ′, the fraction of non-premixed combustion has increased. For the initial increase in the integral scale of mixture distribution (l_{ϕ}), the extent of burning was observed to be increased (compared to the uniformly premixed mixture), followed by a decrease with a further increase in l_{ϕ}. whereas some studies, such as Brearley et al. (2020) reported a reduced flame velocity and flame surface area with increased stratification. With an increase in turbulence, the weakening of this trend was observed. These studies hint towards the non-monotonic behavior of flame propagation with an increase in l_{ϕ} but do not explicitly discuss the potential reason behind this behavior and hence further analysis is required.

The propagation speed of flame in the turbulent medium is calculated by flame displacement speed (S_d). The displacement speed may be defined as the speed of iso-contour of progress variable with respect to the fuel–air mixture. Defining displacement speed based on progress variable (c) is handy in modeling premixed flames. Malkesen and Chakraborty (2010) statistically analyzed displacement speed and compared the change in S_d based on the change in its components, such as reaction (S_r), normal diffusion (S_n), inhomogeneity (S_z), and tangential (S_t). The contribution of the S_z term was observed to be negligible compared to S_d. The S_r and S_n diffusion components were major contributors to S_d. Knowledge of the statistical behavior of S_d is important in modeling a flame. For RANS simulations, the reaction rate closure term is widely modeled by a level set formulation (Tan and Reitz 2006) and the flame surface density (FSD) (Trouve 1994) modeling. These techniques require statistical knowledge of S_d. Understanding the effects of stratification on components of S_d will be useful for efficient modeling of reaction rate closure terms.

In the case of stratified mixture fields, the flame structure can be affected by preferential propagation (Er-Raiy et al. 2020) and the differential diffusion of species. The 3D DNS discussed earlier primarily uses a single-step reaction, approximating the species diffusion with unity Le. Higher flame wrinkling and thinner flame were reported at a lower Lewis number (Le) compared to cases with a higher Lewis number (Suillaud et al. 2022). The quicker flames were observed for mixtures with lower Le values (Patel and Chakraborty 2016). For mixtures with higher Le, difficulties were observed in igniting the mixture compared to lower values of Le. During an analysis of syngas (Hydrogen + Carbon monoxide) combustion, where Hydrogen having $Le \sim 0.3$ and carbon monoxide $Le > 1$, the unity Le assumption may affect the accuracy of the solution.

In the present study, a 2D configuration of DNS is chosen, which allows the inclusion of detailed chemical mechanisms. However, it lacks the precision of 3D DNS because of the inability to include vortex stretching in the solution. The capability of 2D DNS to capture the wrinkling flame structure gives physical relevance to the solution obtained from the simulations. Previously, 2D DNS had been used to calculate the combustion regime (Pal et al. 2017), investigate the curvature effect on premixed combustion (Netzer et al. 2021), and capture the effects of convective mixing of dual-fuel composition (Karimkashi et al. 2020). The 2D DNS has also been used to capture the effects of stratification (Haworth et al. 2000) and the identification of preferential propagation. The studies (Sreedhara and Lakshmisha 2002; Ameen and Abraham 2016) have compared the results of 2D and 3D DNS, and concluded that for qualitative assessment may be carried out with 2D DNS.

The present research is focused on a 2D DNS configuration to understand the physics related to the effect of stratification on S_d. The present study uses the overall lean mixture with a global mean equivalence ratio $< \phi >$ of 0.6. All cases were initialized with same turbulence field to reduce variation across cases due to turbulence. The cases are simulated with a mixture of fields having two values of ϕ' (0.06 and 0.12) and three values of l_{ϕ} / l_{th} (2.5,5, and 10). The present study investigates the effect of l_{ϕ} and ϕ' variation on i) flame propagation and displacement speed of the flame, ii) components of displacement speed. Further the effects of unity *Le* approximation on the displacement speed are studied.

2 Numerical Setup

A 2D DNS with decaying turbulence fields was performed for this study in a domain of 2.4×2.4 cm^2 size. The initial pressure and temperature were kept close to the normal temperature and pressure conditions (1 bar pressure, 300 K temperature). The simulations use PENCIL, an open-source code for compressible reacting flows (Babkovskaia et al. 2011). A sixth-order compact scheme was used for spatial differentiation, and time advancement was performed using low storage RK3 (Runge–Kutta third-order) scheme (Williamson 1980). Periodic boundary conditions were used on all boundaries of the domain. The initial velocity and species fields were imposed with the help of the Passot-Pouquet spectrum (Hinze 1975).

$$E(k) = \frac{32}{3} u' \sqrt{\frac{2}{\pi}} \left(\frac{k^4}{{k_0}^5} \right) \exp\left(-2 \left(\frac{k}{k_0} \right)^2 \right) \tag{1}$$

where u′ is the *rms* of velocity fluctuation, k is wave number, and k_0 is the most energetic wavenumber. Initial auto-correlation between the most energetic scale and initial integral scale L_i is given as

$$k_0 = \frac{1}{L_i \sqrt{2\pi}} \tag{2}$$

An equimolar mixture of H_2 and CO represents syngas, and a chemical mechanism involving 12 species and 38 reactions was used to simulate the combustion of syngas (Davis et al. 2005). A 1D steady-state flame was simulated using PREMIX code (Kee et al. 2000) to calculate flame speed and flame thickness. The laminar flame velocity (S_l) for the 0.6 equivalence ratio was 43.4 cm/s (Reynolds number, $Re = 61$), and flame thickness (l_{th}) was determined by 3 and calculated to be 0.047 cm. An integral scale of 0.11 cm (about twice the l_{th}) was used to impose the initial velocity field. Velocity fluctuations were initialized by imposing a velocity field with u' equal to twice the flame speed and zero mean velocity. A grid of 600×600 cells was chosen to resolve the Kolmogorov length scale using at least two grid points. The flame thickness was resolved using 15 grid points. All cases reported in this paper were simulated for 1.6 ms. The results extracted here are at the instant of 1.25 eddy turn over time (velocity field integral scale/u'). At an instant of 1.6 ms, all flames have crossed critical radius of influence, hence flame propagation is not affected by initial ignition energy.

Karlovitz number (Ka) is defined as $\left(u'/S_l\right)^{3/2}\left(l_{th}/l_t\right)^{1/2}$. Damkohler number ($Da$) is defined as the ratio of the flow time scale (t_f) to the chemical time scale (t_c). here the eddy turnover time is taken as t_f. All cases mentioned here have Ka and Da numbers equal to 1.84 and 1.18, respectively. Therefore, all cases correspond to the thin flame region ($Ka > 1$, $Re > 1$).

$$l_{th} = \frac{T_{\max} - T_{\min}}{(\nabla T)_{\max}} \tag{3}$$

Table 1 Parameters used for the initial distribution of equivalence ratio

Case no	Case	l_ϕ/l_{th}	$\phi'/\bar{\phi}$	$\phi'/\bar{\phi}$(at 1.25 t_f)
1	I0P0	0	0	0
2	I25P1	2.5	0.1	0.070
3	I50P1	5.0	0.1	0.088
4	I100P1	10.0	0.1	0.096
5	I25P2	2.5	0.2	0.141
6	I50P2	5.0	0.2	0.186
7	I100P2	10.0	0.2	0.195

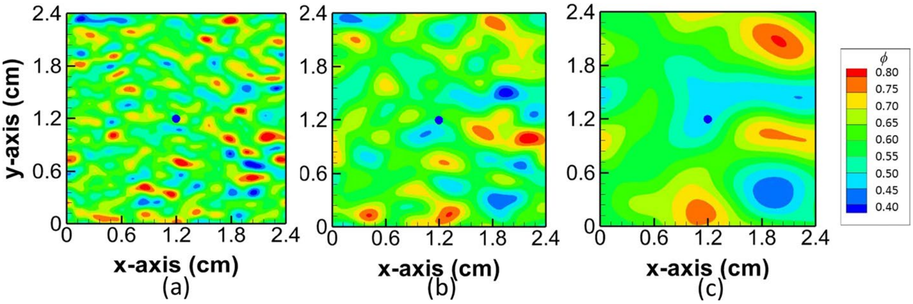

Fig. 1 Initial distribution of equivalence ratio for cases with integral scale equal to (**a**) 0.11 cm (case I25P1), (**b**) 0.22 cm (case I50P1), and (**c**) 0.44 cm (case I100P1)

The effect of the initial equivalence ratio distribution on flame propagation is studied here. For this study, simulations were performed for seven combinations of mixture fields (6 with mixture distribution and 1 with a uniform initial mixture field). The initial ϕ distribution was generated with Eq. 1 (Passot-Pouquet spectrum). For ϕ scalar field, the ϕ' was used instead of $u_{rms,}$ and similar changes were made to find the most energetic wave number based on l_ϕ. The mass fractions of species were assigned based on ϕ value in each cell of the domain. The details of mixture distribution for the cases are summarized in Table 1. The same mixture fields were also solved by artificially forcing unity *Le* for mass diffusivity of all species. The case with the uniform initial mixture is considered case I0P0. The cases with unity Lewis number are named with 1 presiding case name, 1I0P0, 1I25P1, etc.

The initial distributions of equivalence ratios for various l_ϕ are shown in Fig. 1. The hot-spot for flame initiation can be observed at the center of the domain. This table also indicates ϕ′ at the time of observations I,e at *1.25* t_f. From these values of ϕ', it can be observed that higher scalar dissipation rates of lower l_ϕ/l_{th} result in faster dissipation of the mixture distribution field. This faster dissipation results in lower ϕ' values at *1.25* t_f.

The temporal evolution of ϕ field in an unburnt mixture for various cases is shown in Fig. 2. In this figure, the development of the mixture field at *1.25* t_f is compared with the initial distribution for cases with differential diffusion and cases with unity *Le* with help of Probability Density Function (PDF). The PDF help define the density of scattered or continuous variables. Modeling the flame around high-density points of the PDF contributes for enhancing the overall accuracy of the model. The names of the cases are indicated in legends; the number followed after the case name indicates the time

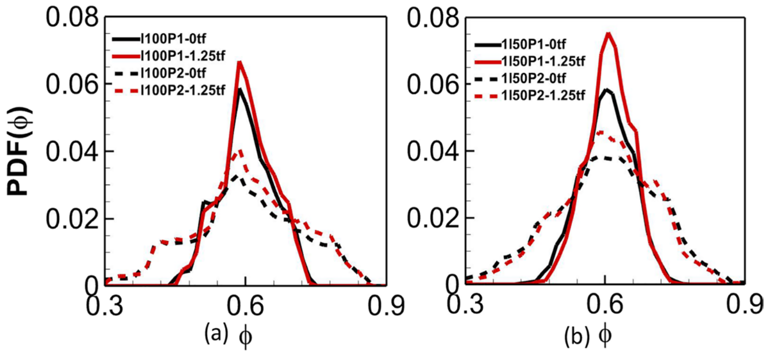

Fig. 2 Temporal evolution of ϕ distribution in the unburnt mixture for cases with **a** differential diffusion, **b** unity Le

instant. From this figure, a narrower spread of ϕ distribution at $1.25\ t_f$ can be observed. At $1.25\ t_f$, Small-scale ϕ-variations dissipate, and the probability of mixture at mean ϕ increases. An increased probability of finding a mixture with ϕ greater than mean ϕ is also observed. The probability of finding higher values of ϕ is observed to increase with an increase in ϕ'. A higher probability of finding large values of ϕ is observed for cases with differential diffusion compared to cases with unity *Le*. Further discussion of these observations is presented in the following sessions.

For stratified combustion, the reaction progress variable based on the Bilger mixture fraction (Peters 1999) is widely used for the analysis. Since the Bilger mixture fraction does not account for species diffusion, a reaction progress variable (c) based on temperature (Richardson and Chen 2017) is adopted in this study; the c value of the cell can be defined as

$$c = \frac{T - T_u}{T_b(Y) - T_u} \tag{4}$$

where T is the temperature of the cell, T_u is the temperature of the unburnt mixture, $T_b(Y)$ is the adiabatic flame temperature of a particular instant for the cell. The PDF of c did not show any significant alteration with the increase in stratification for cases with differential diffusion or unity *Le*. The mixture fraction (ξ) and equivalence ratio (ϕ) were calculated on an element basis.

The diffusion velocities in the species transport equation can be solved by solving full system or approximations such as binary diffusion or multispecies diffusion. Lewis number for species k (Le_k) is defined as

$$Le_k = \frac{\lambda}{\rho C_p D_k} = \frac{D_{th}}{D_k} \tag{5}$$

D_k of a species can be calculated from the value D_{th}. Where D_k is species mass diffusivity, D_{th} is species thermal diffusivity. The Le_k can be artificially selected to find the influence of D_k of species k.

3 Mathematical Formulation

In most practical applications, combustion occurs in turbulent conditions. Numerical solvers such as RANS and LES require models for filtered reaction rates. The widely accepted approaches for closure of reaction rate for premixed and partially premixed mixture, i.e., stratified mixture, are flame surface density (FSD) (Malkeson and Chakraborty 2013) and level set method (Peters 1999) based modeling. In formulations for these closure models, displacement speed (S_d) is a vital parameter. The S_d may be defined as the propagation speed of the scalar iso-surface (progress variable) relative to the fresh mixture (Giannakopoulos et al. 2015). Various research papers have documented the statistical behavior of premixed flame (Chakraborty and Swaminathan 2011; Ozel-Erol et al. 2021); however, studies for the partially premixed mixture are relatively sparse, and results are inconclusive over the range of operating parameters.

For a planar flame with a constant mass flow rate through its entire structure, flame speed takes precise meaning and is called laminar flame speed. Generally, unsteady flame has local curvature and stretch rate at all locations when it propagates inside a turbulent mixture. The definition of laminar flame speed ignores the unsteady behavior and varied mass flow rate across the flame surface. The curvature and stretch rate affect the flame thickness of a propagating flame. In the case of numerical studies, the propagating flame thickness is resolved, and a scalar iso-surface is chosen to analyse flame dynamics. The motion of chosen iso-surface with respect to the fresh reactants represents the motion of the flame. Various progress variables based on scalars, such as temperature, mass fraction, mixture fraction, etc., may be chosen to investigate flame dynamics. Different formulations for displacement speed can be seen in Day et al. (Day et al. 2007). Flame displacement speed can be obtained using Eq. 6.

$$S_d = \frac{1}{|\nabla c|}\frac{Dc}{Dt}\bigg|_{c=c*} = \left(\frac{1}{|\nabla c|}\frac{\partial c}{\partial t} + \frac{v \cdot \nabla c}{|\nabla c|}\right)\bigg|_{c=c*} \tag{6}$$

where v is local gas velocity, the term $-\nabla c/|\nabla c|$ represents the unit normal vector ($\vec{N}$) to propagating flame front. The dot product with local velocity gives local flame velocity normal to the propagating flame front Eq. 6 represents flame speed calculation with respect to flow velocity. The transport equation for scalar c can be written as (Malkeson and Chakraborty 2010)

$$\rho\frac{Dc}{Dt} = \nabla \cdot (\rho D \nabla c) + \dot{\omega}_c + A \tag{7}$$

where D is the mass diffusivity of fuel, $\dot{\omega}_c$ is the reaction rate of progress variable c, which is given in the context of stratified combustion as:

$$\dot{\omega}_c = -\frac{\dot{\omega}_F}{\xi Y_{F\infty}}\, for\, \xi \leqslant \xi_{st} \text{ and } \dot{\omega}_c = -\frac{\dot{\omega}_F\left(1-\xi_{st}\right)}{\xi_{st}(1-\xi)Y_{F\infty}}\, for\, \xi > \xi_{st} \tag{8}$$

where ξ is a mixture fraction, the term 'A' in Eq. 7 denotes the contribution of non-homogeneity in the reactants, which is given as:

$$A = -2\rho D \vec{N} \cdot \nabla\xi|\nabla c|/\xi\, for\, \xi \leqslant \xi_{st} \text{ and } A = -2\rho D \vec{N} \cdot \nabla\xi|\nabla c|/(1-\xi)\, for\, \xi > \xi_{st} \tag{9}$$

The mass diffusivity for the syngas mixture is calculated based on the local mass fraction of the syngas components. From Eq. 7 S_d can be expressed in terms of the component as

$$S_d = \left. \frac{\nabla \cdot (\rho D \nabla c) + \dot{\omega}_c + A}{\rho |\nabla c|} \right|_{c=c*} = S_r + S_n + S_t + S_z \tag{10}$$

The expression for reaction component S_r, normal diffusion component S_n, tangential component S_t and a component corresponding to reactant inhomogeneity S_z for $c = c*$ iso-surface are as follows (Malkeson and Chakraborty 2010)

$$S_r = \left. \frac{\dot{\omega}_c}{\rho |\nabla c|} \right|_{c=c*}, S_n = \left. \frac{\vec{N} \cdot \nabla \left(\rho D \vec{N} \cdot \nabla c \right)}{\rho |\nabla c|} \right|_{c=c*}, S_t = -D\kappa|_{c=c*}, \; S_z = \left. \frac{A}{\rho |\nabla c|} \right|_{c=c*} \tag{11}$$

where κ is the curvature of the flame front and expressed as $\nabla \vec{N}$.

4 Results and Discussion

This section analyzes the effects of stratification on flame growth, flame thickness, and preferential propagation of flame. The effects of stratification in the variation of components of displacement speed S_r, S_n, $S_{t,}$ and S_z within the flame brush and over iso-surface of maximum reaction rate of fuel species are also discussed.

4.1 Effects of Stratification on Flame Surface Growth

The diffusion of reactive species can play a significant role in defining flame behavior. Due to excessive diffusion of H_2 species in the flame front, flame curvature gets modified, and flame propagates quicker in the direction of rich mixture composition (Bhide and Sreedhara 2020). In the case of flame propagation in the stratified mixture, the modification of the flame surface can happen due to differential diffusion (due to non-unity Lewis number) and preferential propagation (due to stratified mixture field). For this reason, a separate set of cases with unity *Le* were also simulated. The cases with $Le = 1$ help separate the effect of differential diffusion from preferential propagation due to stratification. As per the nomenclature, the case name without prefix 1 represents the solution with a combined differential and preferential diffusion effect, and cases with prefix 1 correspond to unity *Le* cases. In the syngas composition, H_2 has $Le < 1$, making it more prone to diffuse into flame, whereas CO has $Le > 1$.

4.1.1 Effect of l_ϕ/l_{th}, ϕ' and $Le = 1.0$ on the Extent of Burning

The approach for measuring the extent of burning was adopted from a numerical study by Patel and Chakraborty (Patel and Chakraborty 2016). The extent of burning is calculated by calculating the area of the domain having $c \geq 0.9$. The effect of stratification on the extent of burning is shown in Fig. 3 by plotting the burnt gas area as a function of time. The extent of burning for stratified cases is compared with that for uniform mixture cases. The names of the cases are given in legends. Figure 3a shows that the flame growth is

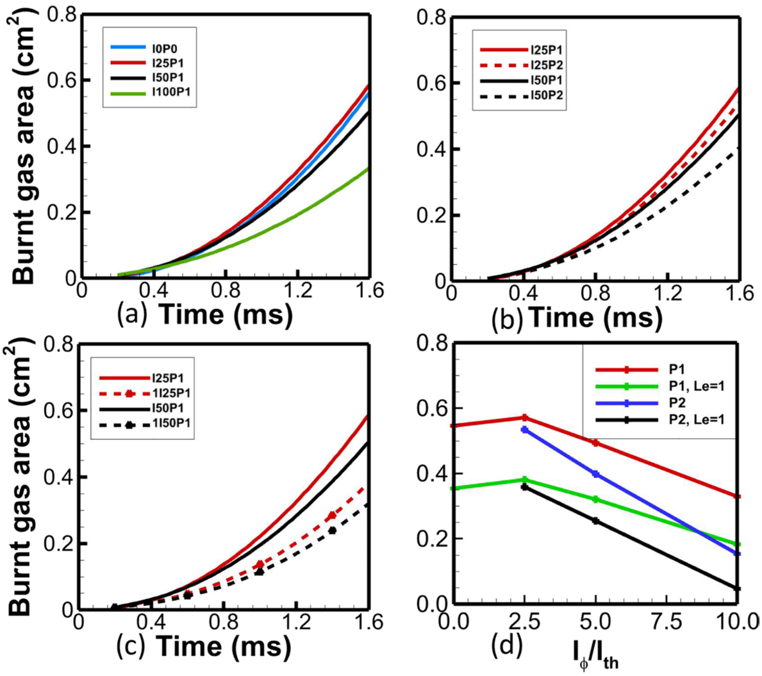

Fig. 3 Evolution of burnt gas area for (**a**) various mixture scales, (**b**) ϕ´, (**c**) comparison of cases with differential diffusion and unity *Le*, and (**d**) variation for various cases at 1.25 t_f The legend represents the names of the cases

reduced as the integral scale of mixing (l_ϕ/l_{th}) increases. Only in case I25P1, where the l_ϕ is close to twice the l_{th}, the flame area growth is rapid compared to the uniform mixture case (I0P0). A similar initial gain in the extent of burning with stratification had been reported previously by Patel and Chakraborty (Patel and Chakraborty 2016). The flame spread is consistently reduced with increased equivalence ratio fluctuation (ϕ'), as shown in Fig. 3b. Figure 3c shows the effect of forcing $Le=1$ to the solution. The results show a considerably lower extent of burning compared to the cases with differential diffusion ($Le \neq 1$) for the same l_ϕ/l_{th}. The similar reduction in consumption rate with increase in Le number has been reported previously (Chakraborty and Swaminathan 2011).

The variation across all listed cases at the instant 1.25 t_f is Fig. 3d. From this figure, it can be seen that cases with $Le=1$ follow a similar trend for the extent of burning as compared to cases with differential diffusion but a slower flame growth is observed for cases with $Le=1$ as compared to non-unity *Le* cases.

4.1.2 Effect of l_ϕ/l_{th}, ϕ' and $Le=1.0$ on Flame Thickness

The flame speed is influenced by the thickness of the flame. It is observed that thinner flame propagates faster than thicker flames (Richardson et al. 2010). The variation in flame thickness (l_{th}) with an increase in stratification is shown in Fig. 4. l_{th} was calculated with the help of Eq. 3, and the adiabatic flame temperature [$T_b(Y)$] was used as T_{max}. From Eq. 3, it can be seen that the flame thickness is inversely proportional to the maximum

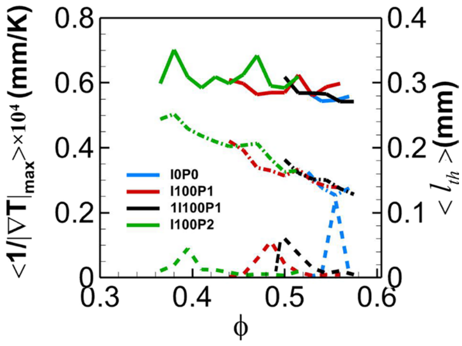

Fig. 4 The conditional average for the inverse of a maximum gradient of temperature (dash dot dash line), flame thickness (solid line) across ϕ. PDF of ϕ distribution is shown as with dashed line

temperature gradient (|∇T|) inside the flame surface. The conditional average of inverse $|\nabla T|_{max}$ and flame thickness across ϕ at1.25 t_f are plotted in Fig. 4. This study was performed at $\phi_{mean} = 0.6$; the mentions of rich and lean packets are based on these ϕ_{mean} values unless otherwise specified. In this figure, it can be observed that $< 1/|\nabla T|_{max} >$ is follows a linear relation with ϕ and inversely proportional to the ϕ. With increased degree of stratification, a reduction in ϕ corresponding to $|\nabla T|_{max}$ location can be observed. The cases with unity *Le* (case 1I100P1) show higher ϕ corresponding to the site of $|\nabla T|_{max}$ than those with differential diffusions for the same mixture distribution. Higher mass diffusivity of fuel component H_2, may have resulted in diffusing H_2 a to high-temperature zones for cases with differential diffusion resulting in lower ϕ at the location of $|\nabla T|_{max}$. The PDF also reveals that with an increase in stratification, the density of $|\nabla T|_{max}$ location shifts towards the lower ϕ values. On the other hand, l_{th} is observed to be slightly reduced with an increase in stratification. Reduction in $T_b(Y)$ with a reduction in ϕ results in a shallower change in l_{th} compared to the change in $1/|\nabla T|_{max}$. It is a well-known fact that flame speed is strongly affected by adiabatic flame temperature of a flame (Law 2006). With an increase in stratification, the flame shifts towards the lean mixture, so even though the changes in flame thickness are negligible, the flame speed is reduced considerably. The cases presented in this study have $\phi_{mean} = 0.6$, Fig. 4 shows a leaner ϕ*'s* at $|\nabla T|_{max}$ locations. For cases with differential diffusion, the reduction in ϕ can be attributed to the higher mass diffusivity of H_2, but the cases with unity *Le* also show similar behavior. This observation indicates that the differential diffusion is not only the reason behind reduced ϕ at locations of $|\nabla T|_{max}$.

4.1.3 Effect of l_ϕ/l_{th}, ϕ′ and *Le* = 1.0 on Preference of Mixture in Preheat Zone

To investigate reduction in ϕ at the location of $|\nabla T|_{max}$ with an increase in stratification, the ϕ-distribution in preheat zone is plotted in Fig. 5. The effect of stratification on the preference of flame propagation was analyzed by plotting PDFs of the temporal evolution of ϕ inside preheat zone for various cases. The evolved fields for higher ϕ' cases are also plotted in this figure. The legends indicate the time instant in terms of t_f of shown distribution, and the number indicated in the bracket corresponds to the case having $\phi'/\phi_{mean} = 0.1$ (1) or $\phi'/\phi_{mean} = 0.2$ (2). The region propagating from $|\nabla T|_{max}$ location up to the unburnt mixture (up to $c = 0.01$) within the flame surface was considered a premix zone (Kortschik et al. 2004).

In Fig. 5a, c (lower l_ϕ/l_{th} cases), the flame is observed to propagate more towards the rich mixture initially at 0.15 t_f. At this instant bimodal distribution of ϕ is observed

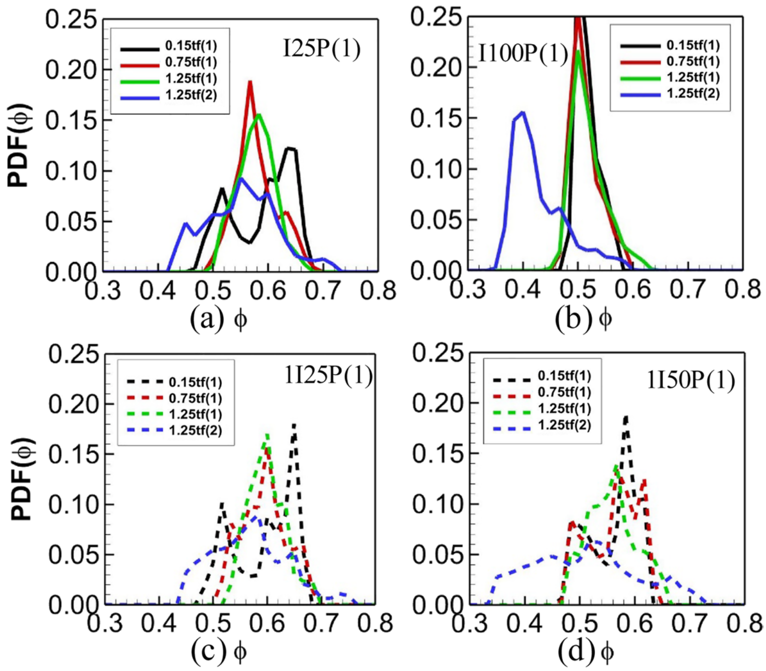

Fig. 5 Temporal evolution of ϕ distribution in preheat zone for **a** case I25P1, **b** case I100P1, **c** case 1I25P1, and **d** case 1I50P1. This number indicated in the bracket of the legend indicates 1 for case with $\phi'/\phi_{mean}=0.1$ and 2 for case with $\phi'/\phi_{mean}=0.2$

with higher density at the rich side can be observed. The excessive energy of the hotspot might be a reason behind this behavior. With further increase in time, the distribution changes from a bimodal to a normal distribution with mean values swiveling around ϕ_{mean}. Whereas cases with higher l_ϕ/l_{th} show a rapid transition of ϕ mode of distribution towards the lean side. The fully evolved profiles for cases with higher ϕ' show similar profiles with values further skewed towards the leaner side of the mixture.

Figure 5 shows that with increased stratification, ϕ distribution in preheat zone is skewed towards the leaner equivalence ratio. A similar preference for propagation in a lean mixture was observed by Pasquier et al. (2007) in their experimental study. In that study, a lack of fuel-rich packets was indicated as the reason for this observation. In another study by Raiy et al. (2020) the presence of inhomogeneity was ascertained as the reason for the accumulation of lean mixtures in front of the flame structure. The probability of finding mixture strength in front of a flame with various mixture strength is also deemed as reason behind this non-monotonic behavior (Patel and Chakraborty 2016). As we have seen earlier in Fig. 2., the field distribution of the unburned mixture fraction shows an increased population for ϕ having value more than ϕ_{mean}. This increased population indicates that the flame preferentially propagates towards a lean mixture even though rich packets are available for combustion. The heat loss from the preheat zone reduces the enthalpy entering into the reaction zone. For a flat burner, the flame was observed to be flexible to adjust its location to the extent of heat transfer (Law 2006). Similar adjustment was also observed in the present study. To analyze

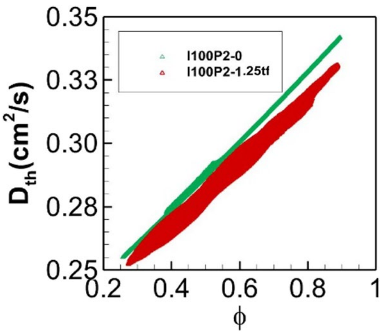

Fig. 6 Scatter plot for variation of thermal diffusivity across ϕ for case I100P2 at instant of 0, and 1.25 t_f

possible reasons behind this preferential behavior the thermal diffusivity (D_{th}) of the mixture available in front of preheat zone is shown in Fig. 6.

Figure 6 shows the variation of thermal diffusivity for unburnt mixture across ϕ distribution. The scatter plot for thermal diffusivity (D_{th}) distribution is plotted for case I100P1 at time instant of 0 and 1.25 t_f. From this figure, it can be observed that D_{th} increases with an increase in ϕ. It is also observed that overall D_{th} values reduced with the progress of time. Compressional heating increased pressure and temperature by 5% and 1.5%, respectively. Higher rise in pressure compared to temperature results in a reduction in D_{th}. The lower values of D_{th} for low ϕ result in heat retention in preheat zone and accelerating oxidation reactions.

The heat from the ignited flame front is used to preheat the mixture in front of the flame. For smaller values of $l_\phi/l_{th,}$ the heat from the flame might have diffused quicker and retained inside a small blob of the rich mixture. That heat might have been sufficient to ignite a small chunk of rich mixture surrounded by lean mixture, resulting in quicker flame propagation than uniformed premixed case. As the size of packets of stratification increases, the heat from the flame front is insufficient to ignite bigger rich packets inside the field, resulting in more combustion at leaner packets where heat is blocked due to the lower D_{th} of the lean mixture. The lean burning again results in lower heat released from the flame front. The larger lean packets result in bigger thermal runaways shifting combustion to the leaner side of the mixture. The mixture with higher ϕ' avails broader compositions in front of the flame. The broader composition spectrum has mixtures with higher and lower values of D_{th}. The availability of high D_{th} further shifts the combustion zone to a lean mixture. For cases with differential diffusion, fuel species H_2 will be diffused into high flame temperature, leaving leaner preheat zones. These leaner flames release less heat and force flame towards a lean mixture where more heat will retain for ignition or combustion.

If the fuel-oxidizer mixture had reversed a trend of D_{th} and ϕ, then the combustion of a mixture can be shifted from a preferentially lean mixture to a rich mixture. The heat released from the flame can determine the value of l_ϕ/l_{th} at which combustion performance can be quicker than premixed or slower than premixed.

4.2 Effects of Stratification on Flame Displacement Speed

The propagation of flame in the turbulent medium can be specified by flame displacement speed (S_d). S_d is defined as the speed of the iso-surface of the flame scalar to the unburnt mixture. S_d can be divided into the components given by Eq. 11 The effects of stratification

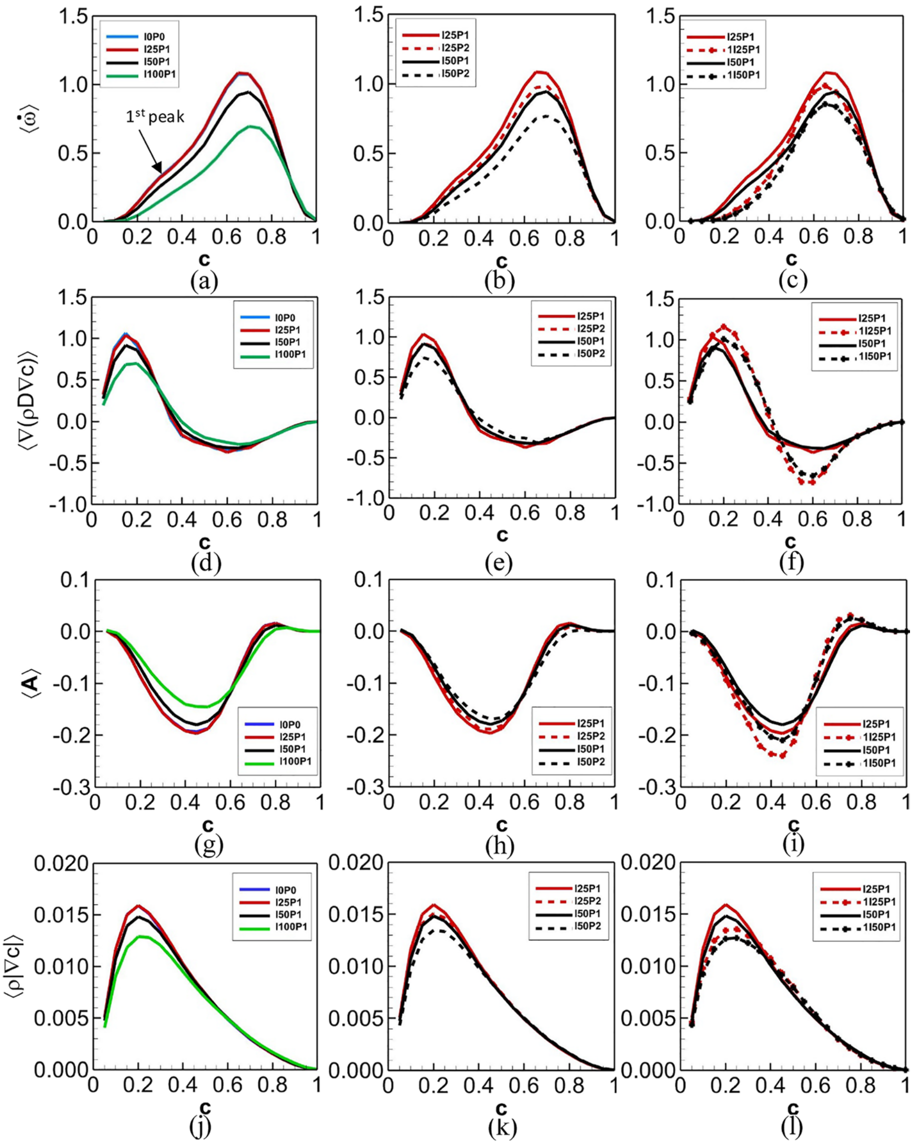

Fig. 7 Variations of components of displacement speed with stratification across the flame surface. The legend represents the names of the cases

on components of S_d averaged over the flame brush ($0.01 < c < 0.99$) can be seen in Fig. 7. In this figure, the average of any quantity (Q) over an iso-surface of c is denoted by $< Q >$. The quantities described in the figure are evaluated over the domain as suggested in the previous study (Malkeson and Chakraborty 2010). These figures show that the contribution of the normal diffusion term ($\langle \nabla(\rho D \nabla c) \rangle$) is positive in the preheat zone and negative at higher progress values. At the same time, reaction terms ($\dot{\omega}$) have positive values everywhere in the domain. The contribution of the inhomogeneity term (A) is negative in the preheat zone and has very low positive values near the c values close to peak reaction rates of fuel species. The conditional mean of the curvature term S_t shows very small values across c, so the results are not discussed here. The terms mentioned in Fig. 7 are not normalized by $\rho|\Delta c|$ as they are in components provided in Eq. 11. From the Fig. 7, it can be observed that flame can have a negative displacement speed when the contributions of S_z, S_t, and S_n overcome the contribution of S_r. The contribution of the inhomogeneity term $<A>$ is observed to be around one tenth of major contributors ($\langle\nabla(\rho D\nabla c)\rangle$, $\dot{\omega}$). The contribution of $<A>$ is also observed near the site of higher values of $\rho|\Delta c|$, this also reduces the contribution of A to the S_d. The negligible values of A are well sync with results observed in previous studies (Malkeson and Chakraborty 2010; Chakraborty 2007). The values of the normal diffusion term are dependent on ∇c, in preheat zone the values as ∇c increases the normal diffusion term is observed to increases. The magnitudes of $\langle\nabla(\rho D\nabla c)\rangle$, $\dot{\omega}$, and $<A>$ is observed to be reduced with increase in stratification. The results are well synced with the previous study (Malkeson and Chakraborty 2010). In that study, the simulations were performed with single step reaction mechanism resulting in peak $\dot{\omega}$ close to $c=0.8$, which is characteristic of single-step reactions. In the present study, the multi-step reaction mechanism resulted in peak $\dot{\omega}$ close to 0.6, indicating a faster reaction rates than single-step reaction mechanism. With a reduction in ϕ, the peak of $\dot{\omega}$ is observed to shift to $c>0.8$. Similar shifting c due to a reduced consumption rate was observed in the study by Veynante et al. (2008).

As the results in the previous section indicate, with an increase in stratification, flame shifts to lower ϕ, resulting in lower values of reaction rates for fuel species. The reduction in reaction rate results in a decrease in $\dot{\omega}$ term. The $\dot{\omega}$ term for cases with differential diffusion shows two peaks. The initial peak (kink) is observed for the peak reaction rates of fuel species H_2 near high-temperature regions and is marked by the arrow in Fig. 7a. This preheating might have helped achieve a larger second peak than unity *Le* cases. The second peak is observed at the location of consumption of CO. From Fig. 7c, it can be observed that for cases with $Le=1$, a single peak with reduced peak values compared to cases with differential diffusion is observed for $\dot{\omega}$ term.

The variation for normal diffusion term with stratification can be observed in Fig. 7d–f. From these figures, it can be observed that with an increase in stratification, gradients of ∇c and normal diffusion term have lower peaks. As we have seen in the earlier section, increased stratification leads to leaner flame. The leaner flame produces lower energy resulting in lower ∇c (Sabelnikov and Lipatnikov 2021). From Fig. 7f it can be observed that the presence of mass diffusivity is responsible for reduction in the magnitude of $\langle\nabla(\rho D\nabla c)\rangle$ term near c^* iso-surface (high temperature). The reduced magnitude of $\langle\nabla(\rho D\nabla c)\rangle$ term for cases with differential diffusion results in higher S_d for same cases compared to cases with $Le=1$. With increase in stratification, the magnitude of the inhomogeneity term ($<$A$>$) also showed similar behavior to $\langle\nabla(\rho D\nabla c)\rangle$ term.

The shifting of flame towards leaner mixture composition with an increase in stratification results in lower magnitudes for all components of S_d. On c^* iso-surface, $\dot{\omega}$ term shows positive values, whereas $\langle\nabla(\rho D\nabla c)\rangle$ and $<A>$ term shows negative values. For cases with differential diffusion magnitude of $\langle\nabla(\rho D\nabla c)\rangle$ and $<A>$ term gets reduced compared to unity *Le* cases. $\dot{\omega}$ term also shows reduced magnitude for $Le=1.0$ cases compared to values for cases with differential diffusion. Due to the reduction magnitude of these two major components, a lower extent of burning is observed in Fig. 3d for unity *Le* cases.

The modeling techniques such as FSD and level-set-based modeling gives utmost importance to the behavior of S_d at a location of maximum reaction rate. Here, the flame location is considered as the iso-surface (c^*) of the maximum reaction rate (Malkeson and

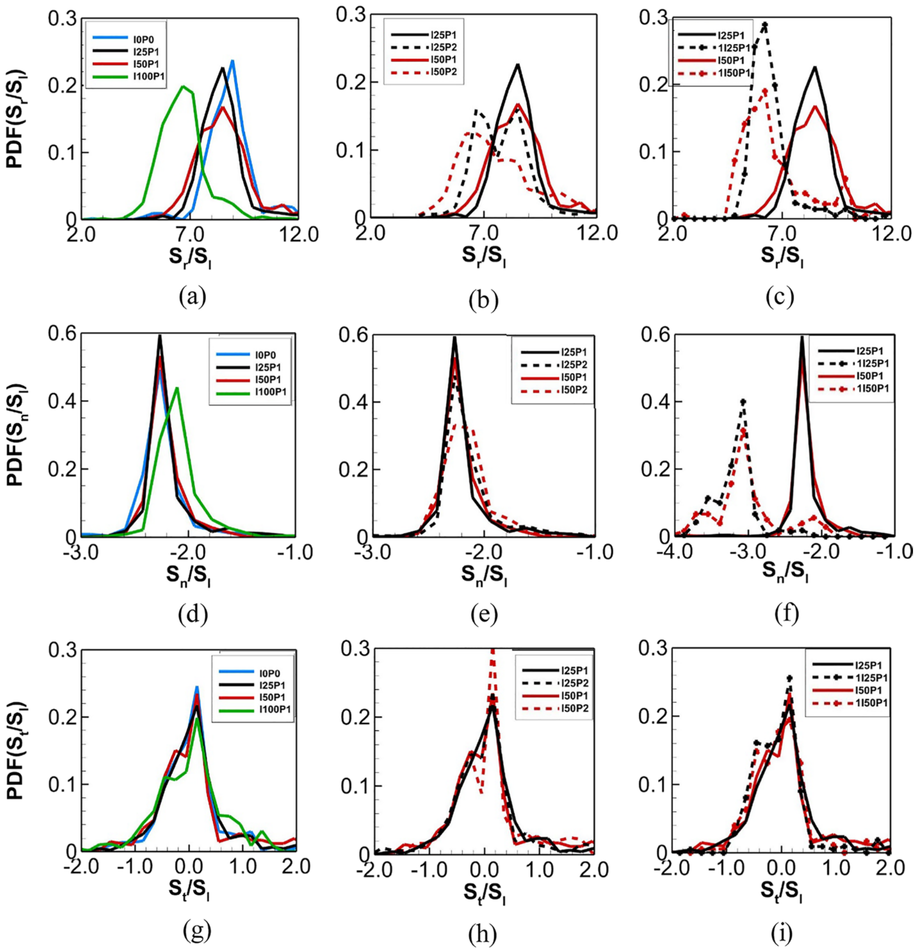

Fig. 8 PDF for components of displacement speed normalized with S_l. The legend represents the names of the cases

Chakraborty 2010). Figure 8 shows the PDF for the S_r, S_n, and S_t components of the displacement speed at the iso-surface of the maximum reaction rate. In previous studies e.g. (Malkeson and Chakraborty 2010), a constant c iso-surface was used to calculate statistics of S_d and its components. In order to reduce the effects of the overlap of flame surfaces in statistics, a very thin flame c^* is selected. The iso-surface with a reaction rate gradient ($\left|\nabla\dot{\omega}_f\right|$) less than 5% of the peak $\left|\nabla\dot{\omega}_f\right|$ is chosen. The S_r, $S_{n,}$ and S_t are major contributors to S_d, so the below results mainly focus on these three components. The S_d and its components values are normalized with the laminar flame speed of syngas at a 0.6 equivalence ratio. The components of S_d show normal distribution, which is in sync with previous studies, e.g., (Er-Raiy et al. 2020).

From Fig. 8a, it can be observed that, with increasing l_ϕ/l_{th}, the peak of S_r distribution reduces to lower values of S_r; the distribution is also observed to become wider with increasing values of l_ϕ/l_{th}. The distribution of S_r is observed to become even wider with an increase in ϕ'. The flame presence at the broader composition of fuel concentration

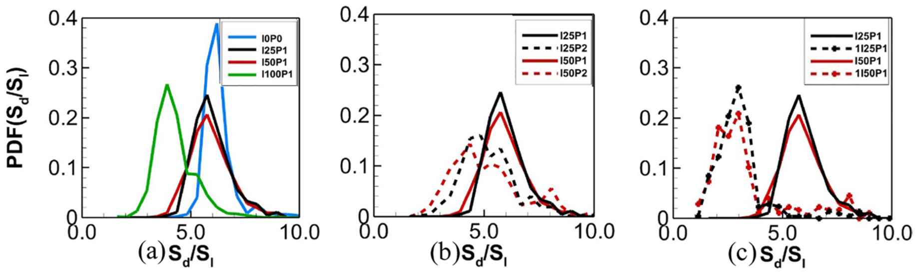

Fig. 9 Probability density functions for displacement speed normalized with S_l at c^* iso-surface. The legend represents the names of the cases

might be a reason behind this widening of the PDF profile. The peak of S_r distribution was also observed to be shifted towards lower values. A similar pattern in results is observed for cases with $Le=1$ (cf. Figure 8c). S_r component is mainly dependent on the reaction rate of fuel components, as we have previously seen the flame preferentially propagate into a lean mixture field, resulting in a lower fuel reaction rate and lower S_r values. The cases with unity Le show a lower peak of $\dot{\omega}$ term than those with differential diffusion. Lower $\dot{\omega}$ term results in lower values of S_r compared to cases with differential diffusion.

The changes in the distribution of S_n over a flame surface can be observed in Fig. 8d–f. For cases with differential diffusion, S_n values attain the same mean with the broader distribution. Due to differential diffusion normal diffusion component shows similar values (cf. Figure 7). The distribution of S_n further widens with an increase in ϕ'. Figure 8f shows the wider distribution profile for S_n with lower valued peaks for cases with $Le=1$. A similar observation from a reactivity point of view was observed previously (Malkeson and Chakraborty 2010); in that study, the magnitude of S_n was reduced with an increase in ϕ. Also, the widening of S_n profile was observed with an introduction of stratification. The lower values observed in Fig. 7 result in lower values S_n in this figure. From Fig. 8g–i, it can be seen that S_t profile widens with an increase in l_ϕ/l_{th}. S_t distribution also becomes bimodal with an increase in ϕ'. The bimodal distribution becomes more pronounced for cases with $Le=1$. The lack of species diffusion in the reaction zone might be a reason behind the bimodal distribution.

The effect of stratification on PDF for cumulated S_d across c^* can be seen in Fig. 9. Figure 9a shows that with the increase in l_ϕ/l_{th}, the distribution of S_d becomes wider. The distribution peak is also observed to be skewed towards lower values. With an increase in ϕ', the PDF further becomes distributed, and the skewed peak towards lower values can be seen in Fig. 9b. The shifting of flame towards the lean ϕ mixture might be a reason behind this behavior. A wider distribution profile with lower peak S_d distribution can be observed for the cases with unity Le. From these results, it can be observed that the S_d for stratification cases shows behavior similar to premixed flames. But, the magnitude of S_d is observed to reduce with increased stratification. The reduced ϕ around the flame with increased stratification reduces the magnitude of S_d. The lower ϕ also shifts peaks for components of S_d to higher c. For cases with unity Le, a reduction is observed in S_r and S_n components resulting in lower S_d compared to cases with differential diffusion.

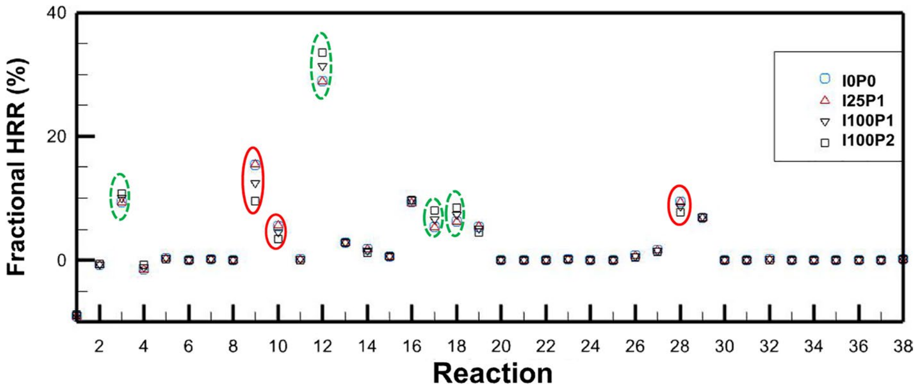

Fig. 10 Share of HRR contribution by individual reaction to net HRR for various cases

Table 2 Major reactions to contribute in HRR

	No	Reaction
Increasing	R3	$OH + H_2 = H + H_2O$
	R12	$H + O_2(+M) = HO_2(+M)$
	R17	$HO_2 + O = OH + O_2$
	R18	$HO_2 + OH = O_2 + H_2O$
Reducing	R9	$H + OH + M = H_2O + M$
	R10	$O + H + M = OH + M$
	R28	$CO + OH = CO_2 + H$

4.3 Effect of Stratification on Reaction's Contribution to HRR

The effects of stratification on the contribution of individual reactions to net HRR are analyzed in this section. The contribution of reactions to HRR for various cases is plotted in Fig. 10. The contributions of reactions shown in the figure are normalized by the total HRR across the flame for each case. The names of cases are given in legends. The selection inside the red markings indicates reactions resulting in reduced HRR contribution with increased stratification, and green selection indicates otherwise for major contributing reactions. The HRR contribution by reaction for unity *Le* cases do not show any significant variations with increased stratifications. The contribution unity *Le* cases for all stratification was observed to be similar to Case I0P0 and hence not discussed here. The negligible variation for cases with $Le = 1$ indicates that the variation in contribution to HRR observed for these reactions is mainly due to the mass diffusion of the species. From this figure, seven major reactions contribute more than 70% of total HRR can be identified. Out of these reactions, the contribution of R3, R12, R17, and R18 increases with stratification. At the same time, the contribution of R9, R10, and R28 decreases with stratification. Reaction nomenclature similar to reaction mechanism is maintained (Davis et al. 2005). These reactions are classified in Table 2. From Fig. 10, it can be observed that R12 is a major contributor to HRR. The contribution of these reactions can be divided into two groups. The variation of these groups across *c* is plotted in Fig. 11.

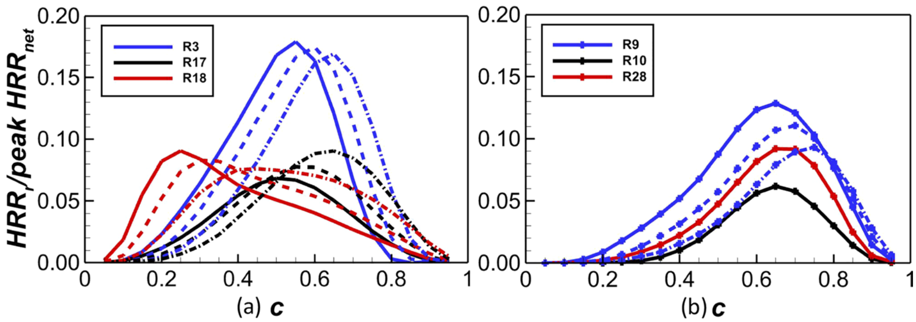

Fig. 11 Variations in reactions contribution to HRR with an increase in stratification for Case I25P1 (Solid line), Case I100P1 (Dotted line), Case I100P2 (Dash Dot line) **a** increased contribution with stratification (Plain line) **b** decreased contribution with stratification (line with symbol)

The values of variation in reaction's contribution to HRR with stratification for major reactions are plotted in Fig. 11. The values of HRR are averaged over *c* and normalized by the peak of the mean HRR plot for each case. R3 and R12 show similar behavior to stratification, so only R3 out of two is plotted in this figure. Here Fig. 11a represents the group of reactions with increasing contribution with stratification, whereas Fig. 11b represents otherwise. All reactions in Fig. 11b show similar behavior to stratification, so only the behavior of R9 is shown in this figure. The reactions classified in Table 2 majorly consume or produce H and OH radicals. As the variation is only observed in cases with differential diffusion, the mass diffusivity of these radicals is analyzed in this section. The variation in budget terms for H and OH terms is shown in Fig. 12. The values shown in this figure are conditioned over *c* and normalized by the peak of a particular quantity near c^*. H and OH species are observed to be produced near c^* and diffused into flame at a lower reaction rate region. The peak of the H species production rate is close to c^*, whereas the peak production rate of the OH species is at higher *c* values. From this Fig. 12 (a-b), it can be observed that with an increase in stratification peak of each budget term shifted to a higher *c* value. Bhide and Sreedhara (Bhide and Sreedhara 2020) observed similar shifting with a reduced heat release rate. This shifting of the peak for budget term results in the narrowing of the production zone. The consumption zone near the preheat zone is observed to thicken, whereas the consumption zone near the burnt gas region is observed to be narrowed.

The widening of the diffusion profile for H and OH species near mid-flame with increased stratification results in higher supply of reactant species for R3, R12, and R18. The increased reactants near the mid of the flame resulted in increased contributions to HRR by these reactions. These reactions also shift their peak HRR values to a higher *c* value (cf. Fig. 11). Narrowing the production zone reduces HRR contributions from reactions R9, R10, and R28. As the reaction R9, R10, and R28 majorly peaked near the production zone of H and OH species.

5 Conclusions

A 2D DNS study is conducted for radially expanding flame inside a stratified medium. The cases with various distributions of the initial mixture fields were simulated with differential diffusion and unity Lewis number (*Le*). An adiabatic flame temperature-based progress

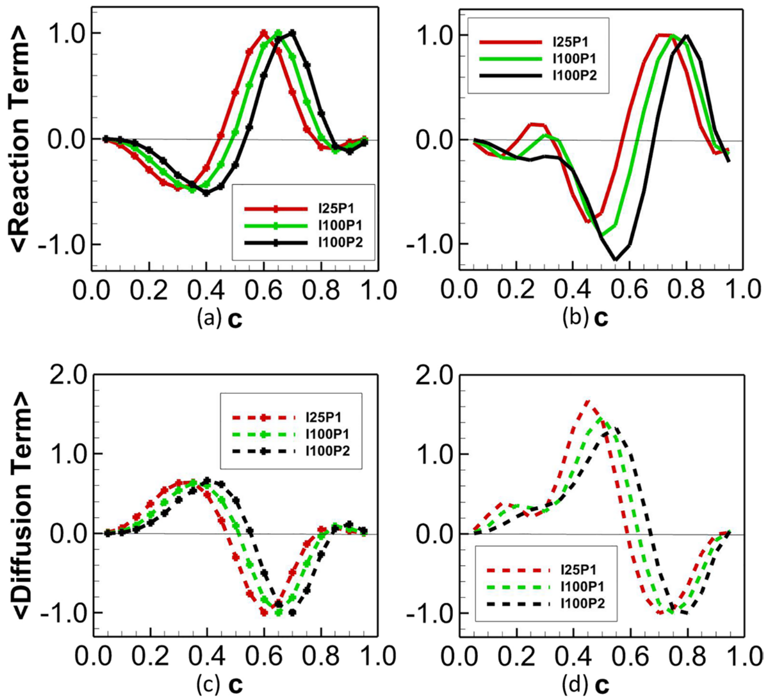

Fig. 12 Variation in conditional averages of Budget terms across c for reaction terms of **a** H, **b** OH and Diffusion terms of **c** H, **d** OH. The values are normalized by peak values of budget terms

variable was used to perform the analysis. The effects of stratification on flame propagation were analyzed in this study. The four component components of S_d were identified, viz. reaction (S_r), normal diffusion (S_n), tangential (S_t), and inhomogeneity (S_z). Among these S_n and S_r are observed to be major contributors to S_d. The results show.

(1) The extent of burning was observed to show a non-monotonic behavior with an increase in the integral scale of mixing (l_ϕ). The higher thermal diffusivity of the rich mixture was observed to provide a thermal runaway for cases with larger l_ϕ. The heat loss from rich packets resulted in the shifting of flame towards the lean mixture compositions. For lower l_ϕ, the enhanced thermal diffusivity was observed to improve the combustion rate for small l_ϕ of stratification, as smaller blobs of mixture inhomogeneity do not lose excessive heat. Further investigation is needed to define optimum l_ϕ for improving the extent of burning.

(2) With the increase in stratification, S_d shows similar trends to mixtures with reduced reactivity due to the shifting of flame towards lean equivalence ratio. S_n shows a significant reduction in cases $Le = 1.0$ compared to cases with differential diffusion. For cases with $Le = 1.0$, reduction in S_r due to the absence of mass diffusivity of H_2 and reduced S_n resulted in significantly lower S_d values compared to cases with differential diffusion.

(3) With the increase in stratification, the peak reaction rate of fuel species (c') was shifted to a higher reaction progress variable (c). The shifting of c' resulted in an alteration of

the diffusion pattern of species across the flame surface. The production zone of H and OH species was narrowed as $c^{'}$ shifted to a larger c value. It reduced the contribution from reactions to HRR, which predominately peaked their HRR near the production zone for H and OH species.

Author Contributions RP and SS wrote manuscript.

Funding Not applicable.

Data Availability Available on request.

Declarations

Conflict of interest The authors declare no competing interests.

Ethical Approval Not applicable.

Informed Consent Not applicable.

References

Agarwal, A.K., Solanki, V.S., Krishnamoorthi, M.: Gasoline compression ignition (GCI) combustion in a light-duty engine using double injection strategy. Appl. Therm. Eng. (2023). https://doi.org/10.1016/j.applthermaleng.2023.120006

Aleiferis, P.G., Hardalupas, Y., Taylor, A.M.K.P., Ishii, K., Urata, Y.: Cyclic variations of fuel-droplet distribution during the early intake stroke of a lean-burn stratified-charge spark-ignition engine. Exp. Fluids **39**, 789–798 (2005). https://doi.org/10.1007/s00348-005-0001-0

Ameen, M.M., Abraham, J.: Are, "2D DNS" results of turbulent fuel/air mixing layers useful for assessing subgrid-scale models? Numer. Heat Transfer Part A Appl. **69**, 1–13 (2016). https://doi.org/10.1080/10407782.2015.1052312

Babkovskaia, N., Haugen, N.E.L., Brandenburg, A.: A high-order public domain code for direct numerical simulations of turbulent combustion. J. Comput. Phys. **230**, 1–12 (2011). https://doi.org/10.1016/j.jcp.2010.08.028

Bai, Y.L., Wang, J.X., Wang, Z., Shuai, S.J.: Knocking suppression by stratified stoichiometric mixture with two-zone homogeneity in a DISI engine. J. Eng. Gas Turbin. Power (2013). https://doi.org/10.1115/1.4005113

Bhide, K.G., Sreedhara, S.: A DNS study on turbulence-chemistry interaction in lean premixed syngas flames. Int. J. Hydrogen Energy **45**, 23615–23623 (2020). https://doi.org/10.1016/j.ijhydene.2020.06.042

Brearley P, Ahmed U, Chakraborty N. The relation between flame surface area and turbulent burning velocity in statistically planar turbulent stratified flames. Physics of Fluids 2020;32. doi:https://doi.org/10.1063/5.0031291.

Chakraborty, N.: Comparison of displacement speed statistics of turbulent premixed flames in the regimes representing combustion in corrugated flamelets and thin reaction zones. Phys. Fluid (2007). https://doi.org/10.1063/1.2784947

Chakraborty, N., Swaminathan, N.: Effects of Lewis number on scalar variance transport in premixed flames. Flow Turb Combust. (2011). https://doi.org/10.1007/s10494-010-9305-0

Cho, Y.S., Santavicca, D.A., Sonntag, R.M.: The effect of spark power on spark-ignited flame kernel growth. SAE Technical Papers (1992). https://doi.org/10.4271/922168 da Costa, R.B.R., Rodrigues Filho, F.A., Coronado, C.J.R., Teixeira, A.F., Netto, N.A.D.: Research on hydrous ethanol stratified lean burn combustion in a DI spark-ignition engine. Appl. Therm. Eng. **139**, 317–324 (2018). https://doi.org/10.1016/j.applthermaleng.2018.05.004

Davis, S.G., Joshi, A.V., Wang, H., Egolfopoulos, F.: An optimized kinetic model of H2/CO combustion. Proc. Combust. Inst. **30**, 1283–1292 (2005). https://doi.org/10.1016/j.proci.2004.08.252

Day, M., Shepherd, I., Bell, J., Grcar, J., Lijewski, M.: Displacement speeds in turbulent premixed flame simulations. Comput. Combust. **2007**, 18–20 (2007)

Er-Raiy, A., Boukharfane, R., Parsani, M.: Effects of composition heterogeneities on flame kernel propagation: a DNS study. Fluids (2020). https://doi.org/10.3390/fluids5030152

Fooladgar, E., Chan, C.K.: Effects of stratification on flame structure and pollutants of a swirl stabilized premixed combustor. Appl. Therm. Eng. **124**, 45–61 (2017). https://doi.org/10.1016/j.applthermaleng.2017.05.197

Giannakopoulos, G.K., Gatzoulis, A., Frouzakis, C.E., Matalon, M., Tomboulides, A.G.: Consistent definitions of “Flame Displacement Speed” and “Markstein Length” for premixed flame propagation. Combust. Flame **162**, 1249–1264 (2015). https://doi.org/10.1016/j.combustflame.2014.10.015

Haworth, D.C., Blint, R.J., Cuenot, B., Poinsot, T.J.: Numerical simulation of turbulent propane-air combustion with nonhomogeneous reactants. Combust. Flame **121**, 395–417 (2000). https://doi.org/10.1016/S0010-2180(99)00148-0

Hinze, J.O.: Turbulence. McGraw-Hill Book Co., New York (1975)

Ilbas, M., Karyeyen, S.: Experimental analysis of premixed and non-premixed methane flames by using a new combustion system. Res. Eng. Struct. Mater. (2017). https://doi.org/10.17515/resm2016.61en714

Jiménez, C., Cuenot, B., Poinsot, T., Haworth, D.: Numerical simulation and modeling for lean stratified propane-air flames. Combust. Flame **128**, 1–21 (2002). https://doi.org/10.1016/S0010-2180(01)00328-5

Kang, T., Kyritsis, D.C.: Methane flame propagation in compositionally stratified gases. Combust. Sci. Technol. **177**, 2191–2210 (2005). https://doi.org/10.1080/00102200500240836

Karimkashi, S., Kahila, H., Kaario, O., Larmi, M., Vuorinen, V.: A numerical study on combustion mode characterization for locally stratified dual-fuel mixtures. Combust. Flame **214**, 121–135 (2020). https://doi.org/10.1016/j.combustflame.2019.12.030

Kee, R.J., Rupley, F.M., Miller, J.A., Coltrin, ME., Grcar, J., Meeks, H. et al.: CHEMKIN Collection, Release 3.6. San Diego, CA (2000).

Kortschik, C., Plessing, T., Peters, N.: Laser optical investigation of turbulent transport of temperature ahead of the preheat zone in a premixed flame. Combust. Flame **136**, 43–50 (2004). https://doi.org/10.1016/j.combustflame.2003.09.018

Law, C.K.: Combustion Physics. Cambridge University Press, New York (2006)

Malkeson, S.P., Chakraborty, N.: Statistical analysis of displacement speed in turbulent stratified flames: a direct numerical simulation study. Combust. Sci. Technol. **182**, 1841–1883 (2010). https://doi.org/10.1080/00102202.2010.500993

Malkeson, S.P., Chakraborty, N.: Statistical analysis and a-priori modelling of flame surface density transport in turbulent stratified flames: a direct numerical simulation study. Flow Turbul. Combust. **90**, 143–187 (2013). https://doi.org/10.1007/s10494-012-9435-7

Manente, V., Johansson, B., Cannella, W.: Gasoline partially premixed combustion, the future of internal combustion engines? Int. J. Engine Res. **12**, 194–208 (2011). https://doi.org/10.1177/1468087411402441

Netzer, C., Ahmed, A., Gruber, A., Løvås, T.: Curvature effects on NO formation in wrinkled laminar ammonia/hydrogen/nitrogen-air premixed flames. Combust. Flame **232**, 111520 (2021). https://doi.org/10.1016/j.combustflame.2021.111520

O’Donnell, P.C., Lawler, B., Lopez-Pintor, D., Sofianopoulos, A.: Effects of injection pressure and timing on low load low temperature gasoline combustion using LES. Appl. Therm. Eng. **232**, 121001 (2023). https://doi.org/10.1016/j.applthermaleng.2023.121001

Ozel-Erol, G., Klein, M., Chakraborty, N.: Lewis number effects on flame speed statistics in spherical turbulent premixed flames. Flow Turbul. Combust. **106**, 1043–1063 (2021). https://doi.org/10.1007/s10494-020-00173-7

Pal, P., Valorani, M., Arias, P.G., Im, H.G., Wooldridge, M.S., Ciottoli, P.P., et al.: Computational characterization of ignition regimes in a syngas/air mixture with temperature fluctuations. Proc. Combust. Inst. **36**, 3705–3716 (2017). https://doi.org/10.1016/j.proci.2016.07.059

Pasquier, N., Lecordier, B., Trinité, M., Cessou, A.: An experimental investigation of flame propagation through a turbulent stratified mixture. Proc. Combust. Inst. **31**, 1567–1574 (2007). https://doi.org/10.1016/j.proci.2006.07.118

Patel, D., Chakraborty, N.: Localised forced ignition of globally stoichiometric stratified mixtures: a numerical investigation. Combust. Theor. Model. **18**, 627–651 (2014). https://doi.org/10.1080/13647830.2014.959456

Patel, D., Chakraborty, N.: Effects of fuel lewis number on localised forced ignition of globally stoichiometric stratified mixtures: a numerical investigation. Flow Turbul. Combust. **96**, 1083–1105 (2016). https://doi.org/10.1007/s10494-015-9692-3

Peters, N.: The turbulent burning velocity for large-scale and small-scale turbulence. J. Fluid Mech. **384**, 107–132 (1999). https://doi.org/10.1017/S0022112098004212

Richardson, E.S., Chen, J.H.: Analysis of turbulent flame propagation in equivalence ratio-stratified flow. Proc. Combust. Inst. **36**, 1729–1736 (2017). https://doi.org/10.1016/j.proci.2016.06.140

Richardson, E.S., Granet, V.E., Eyssartier, A., Chen, J.H.: Effects of equivalence ratio variation on lean, stratified methane-air laminar counterflow flames. Combust. Theor. Model. **14**, 775–792 (2010). https://doi.org/10.1080/13647830.2010.490881

Sabelnikov, V.A., Lipatnikov, A.N.: Scaling of reaction progress variable variance in highly turbulent reaction waves. Phys. Fluids (2021). https://doi.org/10.1063/5.0059938

Sreedhara, S., Lakshmisha, K.N.: Autoignition in a non-premixed medium: DNS studies on the effects of three-dimensional turbulence. Proc. Combust. Inst. **29**, 2051–2059 (2002). https://doi.org/10.1016/S1540-7489(02)80250-4

Suillaud, E., Truffin, K., Colin, O., Veynante, D.: Direct Numerical Simulations of high Karlovitz number premixed flames for the analysis and modeling of the displacement speed. Combust. Flame **236**, 111770 (2022). https://doi.org/10.1016/j.combustflame.2021.111770

Tan, Z., Reitz, R.D.: An ignition and combustion model based on the level-set method for spark ignition engine multidimensional modeling. Combust. Flame **145**, 1–15 (2006). https://doi.org/10.1016/j.combustflame.2005.12.007

Tan, J.Y., Bonatesta, F., Ng, H.K., Gan, S.: Developments in computational fluid dynamics modelling of gasoline direct injection engine combustion and soot emission with chemical kinetic modelling. Appl. Therm. Eng. **107**, 936–959 (2016). https://doi.org/10.1016/j.applthermaleng.2016.07.024

Telli, G.D., Zulian, G.Y., Lanzanova, T.D.M., Martins, M.E.S., Rocha, L.A.O.: An experimental study of performance, combustion and emissions characteristics of an ethanol HCCI engine using water injection. Appl. Therm. Eng. **204**, 118003 (2022). https://doi.org/10.1016/j.applthermaleng.2021.118003

Trouve, A.: The evolution equation for the flame surface density in turbulent premixed combustion. J. Fluid Mech. **278**, 1–31 (1994). https://doi.org/10.1017/S0022112094003599

Veynante, D., Fiorina, B., Domingo, P., Vervisch, L.: Using self-similar properties of turbulent premixed flames to downsize chemical tables in high-performance numerical simulations. Combust. Theor. Model. **12**, 1055–1088 (2008). https://doi.org/10.1080/13647830802209710

Williamson, J.H.: Low-storage Runge-Kutta schemes. J. Comput. Phys. **35**, 48–56 (1980). https://doi.org/10.1016/0021-9991(80)90033-9

Zhao, W., Qiu, P., Liu, L., Shen, W., Lyu, Y.: Combustion and NOx emission characteristics of dual-stage lean premixed flame. Appl. Therm. Eng. **160**, 113951 (2019). https://doi.org/10.1016/j.applthermaleng.2019.113951

Zhou, J., Nishida, K., Yoshizaki, T., Hiroyasu, H.: Flame propagation characteristics in a heterogeneous concentration distribution of a fuel-air mixture. SAE Technical Papers 1440–60 (1998)